Front. Environ. Sci. Eng. 2024, 18(11): 139
https://doi.org/10.1007/s11783-024-1899-x

RESEARCH ARTICLE

Aquatic photo-transformation and enhanced photoinduced toxicity of ionizable tetracycline antibiotics

Linke Ge[1,2], Jinshuai Zheng[1], Crispin Halsall[2], Chang-Er Chen[3], Xuanyan Li[1], Shengkai Cao[2], Peng Zhang (✉)[1]

1 School of Environmental Science and Engineering, Shaanxi University of Science & Technology, Xi'an 710021, China
2 Lancaster Environment Centre, Lancaster University, Lancaster LA1 4YQ, UK
3 Environmental Research Institute/School of Environment, South China Normal University, Guangzhou 510006, China

HIGHLIGHTS

- Mechanisms for multiple photochemical transformation of tetracyclines were reported.
- The degradation kinetics were dependent on pH and reactivities of dissociated forms.
- Anionic forms reacted faster in the apparent photolysis and photooxidation processes.
- Different pathways and various intermediates occurred for the three reactions.
- The major by-products showed similar or more toxicities than the parent antibiotics.

ARTICLE INFO

Article history:
Received 5 February 2024
Revised 7 May 2024
Accepted 6 August 2024
Available online 11 September 2024

Keywords:
Tetracyclines
Dissociation
Photodegradation kinetics
Reactive oxygen species
Transformation products
Risks

GRAPHIC ABSTRACT

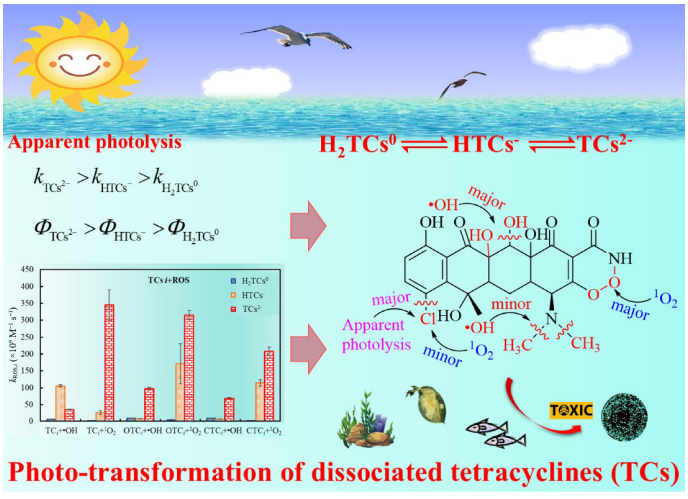

ABSTRACT

Most antibiotics contain ionizable groups that undergo acid-base dissociation giving rise to diverse dissociated forms in aquatic systems depending on the pH of the system. In sunlit surface waters, photochemical transformation plays a crucial role in determining the fate of antibiotics. This study presents a comprehensive examination of the photo-transformation degradation kinetics, pathways and photoinduced toxicity of three widely detected tetracyclines (TCs): tetracycline (TC), oxytetracycline (OTC), and chlortetracycline (CTC). Under simulated sunlight ($\lambda > 290$ nm), their apparent photolysis followed pseudo-first-order kinetics, with rate constants significantly increasing from H_2TCs^0 to TCs^{2-}. Through competition kinetic experiments and matrix calculations, it was found that the anions $HTCs^-$ or TCs^{2-} (pH ~ 8–10) were more reactive toward hydroxyl radicals (•OH), while TCs^{2-} (pH ~ 10) reacted the fastest with singlet oxygen ($^1O_2$). Considering the dissociated species, the total environmental photo-transformation half-lives of TCs were determined, revealing a strong dependence on the water pH and seasonal variation in sunlight. Generally, apparent photolysis was the dominant photochemical process, followed by $^1O_2$ and •OH oxidation. Different transformation pathways for the three reactions were determined based on the key photoproducts identified using HPLC-MS/MS. Toxicity tests and ECOSAR software calculations confirmed that the intermediates produced by the •OH and $^1O_2$ photo-oxidation processes were more toxic than the parent compounds. These findings significantly enhance our understanding of the complex photochemical fate and associated risks of TCs in aqueous environments.

✉ Corresponding author
E-mail: zhangpeng4477@sust.edu.cn

1 Introduction

Antibiotics have emerged as a growing concern in both freshwater and coastal environments due to their frequent detection, pseudo-persistence, and the escalating issue of antimicrobial resistance (Guo et al., 2020; Wang et al., 2022; Zheng et al., 2023). These substances primarily enter ecosystems through animal/human excretion and discharge into wastewater systems, stemming from applications in human medicine, animal husbandry, and aquaculture (He et al., 2020; Ye et al., 2022; Yu et al., 2022; Li et al., 2023). Despite advances in wastewater treatment technologies, these facilities often fail to completely remove antibiotics, leading to residual amounts in receiving waters (Anjali and Shanthakumar, 2019; Ping et al., 2022). Among various antibiotic classes, tetracycline antibiotics (TCs) are consistently identified as noteworthy aqueous micropollutants, frequently found in surface waters in many countries such as the United States, Vietnam, and China (Zhang et al., 2013; Tran et al., 2019; Liu et al., 2020; Xu et al., 2021a). In China, monitoring studies have recorded mean TCs concentrations ranging from 1.42 to 273 ng/L in the aquatic environment (Li et al., 2018; Liu et al., 2018; Zhang et al., 2023) (Fig. A1). Alarmingly, many of these observed concentrations exceed their predicted levels that are safe for aquatic organisms (An et al., 2015; Zhang et al., 2019). To comprehensively grasp the fate and risk of antibiotics, particularly TCs, in surface waters, it is imperative to understand their transformation and fate in aquatic systems as well as the toxicity (Cheng et al., 2019; Hu et al., 2024).

In surface waters, the transformation of antibiotics primarily occurs through photodegradation and biodegradation (Knapp et al., 2005; Ge et al., 2010; Ge et al., 2019). However, the biodegradation can be hindered by factors such as heavy metals, salinity, and pH (Adamek et al., 2016; Yuan et al., 2023). Conversely, sunlight-induced photodegradation, including apparent photolysis and photooxidative degradation induced by reactive oxygen species (ROS), has been identified as the predominant pathway (Li et al., 2016; Felis et al., 2022; Zhang et al., 2022a). TCs, including tetracycline (TC), oxytetracycline (OTC), and chlortetracycline (CTC), can undergo apparent photolysis with degradation rates strongly influenced by pH (Werner et al., 2006; Niu et al., 2013; Song et al., 2020). In addition, TCs are subject to indirect photolysis initiated by photoinduced ROS (e.g., •OH, $^1O_2$, and $O_2^{\bullet-}$), following the pH-dependent second-order reaction kinetics (Werner et al., 2006; Jiao et al., 2008a; Niu et al., 2013). These studies established a solid foundation for further exploration into how pH influences the photo-transformation kinetics of TCs. Given the ionizable groups in their molecular structures (e.g., $-NH_n$ and −OH), many TCs undergo acid-base dissociation depending on environmental pH values. This dissociation significantly affects their degradation processes, necessitating a comprehensive evaluation of the impact of these transformations under varying pH, typically ranging from 6 to 9 in surface waters. It is therefore useful to quantify the photo-transformation kinetics of the different dissociated forms of TCs (H_2TCs^0, $HTCs^-$, and TCs^{2-}) but also to extrapolate the laboratory data to the real-world environment to accurately assess the environmental photochemical fate of TCs.

Previous studies have highlighted the photomodified toxicity and photoenhanced antibacterial activity of many antibiotics, raising concerns about their impact on aquatic microorganisms (Jiao et al., 2008a; Ge et al., 2018). For instance, TC has been shown to photo-transform into by-products that exhibit increased toxicity to *Vibrio fischeri* (Han et al., 2020; Park et al., 2023). In pure water, the photolysis photoproducts of TC and OTC arose through the removal of $-NH_2$, –OH and $-CH_3$ moieties (Oka et al., 1989; Jiao et al., 2008b). Moreover, these antibiotics primarily underwent addition reactions with •OH while experiencing oxidation reactions when reacting with $^1O_2$ (Chen and Huang, 2011; Chen et al., 2011). However, information on the photoproducts of CTC and its •OH and $^1O_2$-initiated photooxidation is still limited, and the distinctions in products and pathways among these reactions remain unclear. Therefore, for a more comprehensive assessment of their ecological fate and risk, it is essential to elucidate the diverse transformation pathways and the resultant changes in toxicity following photodegradation.

This study aimed to explore the kinetics, pathways, and photoinduced toxicity associated with the multivariate photo-transformation reactions of TCs, including both apparent photolysis and oxidation reactions mediated by ROS (e.g., •OH and $^1O_2$) in aqueous environments. Three TCs (i.e., TC, OTC, and CTC) were selected because they are widely present in surface waters (Qi et al., 2018; Xu et al., 2021a; Su et al., 2023) (Table A1). We quantified the multivariate photo-transformation kinetics for the different dissociated forms of the three TCs (H_2TCs^0, $HTCs^-$, and TCs^{2-}). Additionally, we conducted a thorough investigation and comparison of the various photo-transformation products and pathways of CTC, including an assessment of the toxicities associated with its individual photoproducts. CTC is of great concern as a chlorinated organic compound because of its complex biological effects (Riu et al., 2011; Tian et al., 2024). The findings from the present study will provide crucial insights for accurately evaluating the fate and photochemical risk of dissociable antibiotics in aquatic environments.

2 Materials and methods

2.1 Reagents and materials

The three TCs, including TC, OTC, and CTC (purity >

98%), were purchased from J&K, USA, and their chemical structures are shown in Table A2. Hydrogen peroxide (H_2O_2, 30%), *p*-nitroanisole (PNA, 97%), and benzophenone (97%) were obtained from the different suppliers, referring to our previous studies (Ge et al., 2018; Ge et al., 2019). Acetonitrile, acetophenone (AP), furfuryl alcohol (FFA, 98%), and pyridine (Pyr) were of HPLC grade. Other reagents, such as HCl and NaOH, were analytical grade, and ultrapure water was prepared by the Millipore-Milli Q system.

2.2 Photochemical experiments

2.2.1 Apparent photolytic kinetic experiments

Photolysis experiments were carried out using a merry-go-round photochemical reactor (Fig. A2). The light source was a 500 W high-pressure mercury lamp with a water-cooled Pyrex well, of which the light intensities at the reaction solutions were 1.98 and 1.83 mW/cm^2, respectively, at 365 and 420 nm. Mercury lamps filtered by Pyrex glass are often used to simulate sunlight irradiation (λ > 290 nm) (Sciscenko et al., 2021; Xu et al., 2021b; Zhou et al., 2021; Zhang et al., 2022b). The reaction solutions (5 μmol/L) were poured into quartz tubes (50 mL), and the solution pH was adjusted with HCl/NaOH to investigate the photolysis kinetics at pH = 6, 8, and 10. The experimental temperature was controlled at 25 ± 1 °C. PNA/Pyr was used as an actinometer to determine the quantum yield (Φ) according to Eq. (1),

$$\Phi_s = \frac{k_s}{k_a}\frac{\Sigma L_\lambda \varepsilon_{\lambda,a}}{\Sigma L_\lambda \varepsilon_{\lambda,s}}\Phi_a, \quad (1)$$

where a and s represent the actinometer and substrates (TCs), respectively; the quantum yield Φ_a = 0.44 C_{Pyr} + 0.00028; k is the photochemical reaction rate constant (min^{-1}); L_λ is the light intensity of the light source at wavelength λ (mW/cm^2). All the experiments were repeated at least in triplicate with the dark controls.

2.2.2 Determination of ROS oxidation reactivities

Competition kinetics experiments were carried out to examine the oxidation reactivities of TCs with ROS. H_2O_2 (100 μmol/L) and perinaphthenone (20 μmol/L) were used as the photosensitizers to generate •OH and $^1O_2$, respectively. The corresponding reference compounds were AP (10 μmol/L) and FFA (20 μmol/L). To avoid the apparent photodegradation of the reference compounds and TCs (Fig. A3), 410 nm cut-off filters were employed to adjust the emission spectra of the same light source (λ > 410 nm). After sampling at predetermined intervals (0, 15, 30, 60, and 90 min), methanol or NaN_3 was added quantitatively to quench excess •OH or $^1O_2$ to prevent TCs from continuing to react. The bimolecular reaction rate constants $k_{ROS,TCs}$ ($k_{•OH,TCs}$ and $k_{^1O_2,TCs}$) of TCs with •OH and $^1O_2$ were calculated by Eq. (2),

$$k_{ROS,TCs} = \frac{\ln([TCs]_t/[TCs]_0)}{\ln([R]_t/[R]_0)}k_{ROS,R}, \quad (2)$$

where $k_{ROS,R}$ is the second-order rate constant of the reference (R), $k_{•OH,AP}$ = 5.9 × 10^9 L/(mol·s), $k_{^1O_2,FFA}$ = 1.2 × 10^8 L/(mol·s).

2.3 Analytical determinations

The concentrations of TCs were quantified by Waters Ultra-High Performance Liquid Chromatography (UPLC) equipped with a BEHC18 column (2.1 mm × 50 mm, 1.7 μm). The Waters Oasis HLB solid-phase extraction columns (WAT106202) were used to enrich the photo-transformation products. Then, the products were identified using the Agilent 6400 LC-MS/MS with electrospray ionization (ESI) in positive ion monitoring mode. The detailed instrument parameters were listed in the supplementary information (Table A3).

2.4 Acute toxicity test

Following an international standard method (ISO11348-3-2007), luminescent bacteria (*Vibrio fischeri*) were selected to investigate the 15-min acute toxicities of CTC solutions during degradation. A water-quality detector (USA HACH Eclox) recorded luminous intensities. Each sample was tested in triplicate, and the luminescence inhibition rates were calculated according to our previous studies (Ge et al., 2015; 2018). Significant differences in the calculated results was evaluated by a one-way analysis of variance (SPSS version 27.0). Furthermore, based on the degradation-product structures identified with LC-MS/MS, the toxicities of these individual products to aquatic organisms such as fish, daphnia, and green algae were evaluated using ECOSAR v2.0 toxicity prediction software.

3 Results and discussion

3.1 Apparent photolysis kinetics and quantum yields

In the dark-control experiments, no significant degradation (p > 0.1) of the three TCs was observed. Upon exposure to simulated solar irradiation, significant degradation of all the target compounds were observed (p < 0.05), suggesting that photolysis plays a crucial role in their breakdown in aquatic environments. Taking OTC as an example, the fitted curves for the apparent photolysis kinetics under different pH conditions are shown in Fig. 1. The correlation coefficients R^2 are greater than 0.95, indicating that the photochemical reaction followed pseudo-first-order reaction kinetics.

Furthermore, it was found that the photolysis rate constants (k_{TCs}) increased with increasing pH values (Table A4). The increase in photolysis rates with pH was also observed in previous studies (Jiao et al., 2008a; Jin et al., 2017). According to Fig. A4, the pH dependence of k_{TCs} is attributed to the diverse array of dissociated species of TCs (H_2TCs^0, $HTCs^-$, and TCs^{2-}) under different pH conditions.

Furthermore, the photolytic rate constants, k_i, for the dissociated species of TCs (i.e., $k_{H_2TCs^0}$, k_{HTCs^-}, and $k_{TCs^{2-}}$) were calculated using a matrix approach encapsulated in Eq. (3),

$$\begin{matrix}\text{pH=6}\\ \\ \text{pH=10}\end{matrix}\begin{pmatrix}\delta_{H_2TCs^0} & \delta_{HTCs^-} & \delta_{TCs^{2-}}\\ \vdots & \vdots & \vdots\\ \vdots & \vdots & \vdots\\ \vdots & \vdots & \vdots\end{pmatrix}\begin{pmatrix}k_{H_2TCs^0}\\ k_{HTCs^-}\\ k_{TCs^{2-}}\end{pmatrix}=\begin{pmatrix}k_{TCs}\\ \vdots\\ \vdots\\ \vdots\end{pmatrix}\begin{matrix}\text{pH=6}\\ \\ \text{pH=10}\end{matrix} \quad (3)$$

where δ_i represents the proportion of each dissociated form (H_2TCs^0, $HTCs^-$, and TCs^{2-}). The results, detailed in Table 1, reveal a significant increase in k_i from H_2TCs^0 to TCs^{2-}. Moreover, the corresponding Φ_i of the dissociated species was determined (Table 1), which showed the highest photolytic efficiency of TCs^{2-}, followed by that of $HTCs^-$ and H_2TCs^0. Similar to TCs, most sulfonamide antibiotics (SAs) underwent more efficient photodegradation in their anionic forms (SAs^-) (Ge et al., 2019). However, fluoroquinolone antibiotics (FQs) exhibited a different order of photolytic efficiencies: $\Phi_{HFQs^0} > \Phi_{H_2FQs^+} > \Phi_{FQs^-}$ (Ge et al., 2018). These differences highlight the unique reactivities dependent on the dissociated species across various classes of antibiotics, suggesting that molecular structure and ionic state significantly influence the environmental fate of these compounds.

Theoretically, the k of organic compounds in optically transparent solutions can be expressed by Eq. (4) (Werner et al., 2006),

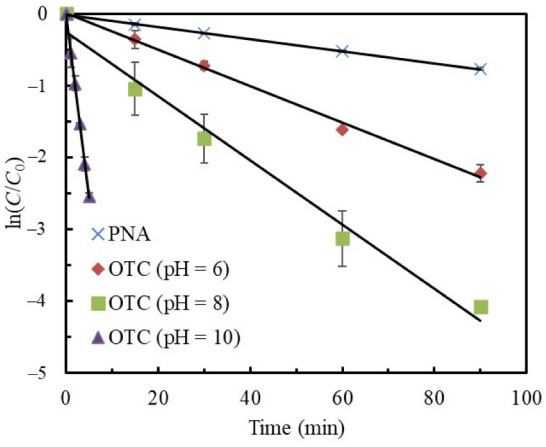

Fig. 1 Apparent photodegradation kinetics of oxytetracycline (OTC) under different pH conditions and *p*-nitroanisole (PNA) in pure water.

$$k = 2.303\Phi\Sigma(L_\lambda\varepsilon_\lambda), \quad (4)$$

where L_λ represents the light intensity and ε_λ is the molar extinction coefficient. It can be seen from Eq. (4) that the k values mainly depend on $\Sigma(L_\lambda\varepsilon_\lambda)$ and Φ. As shown in Fig. A5, the $\Sigma(L_\lambda\varepsilon_\lambda)$ values for the dissociated species of TCs do not change significantly ($p > 0.1$). In contrast, the Φ_i values vary considerably ($p < 0.05$), indicating that Φ_i is an important factor for determining the photolysis rate of TCs in different dissociated forms.

3.2 Photooxidation kinetics and ROS reactivities

No obvious degradation ($p > 0.1$) of the three TCs was found in the control experiments. However, TCs degraded to varying degrees through reacting with •OH and $^1O_2$ in the competition kinetics experiments. Their corresponding bimolecular reaction rate constants ($k_{ROS,TCs}$) are listed in Table A5. The $k_{\bullet OH,TCs}$ of TCs are of the same order of magnitude (10^9) of other classes of antibiotics, such as SAs (Ge et al., 2019), FQs (Ge et al., 2015) as well as furans (Edhlund et al., 2006), and triclosan (Latch et al., 2005). However, in comparison to various classes

Table 1 Apparent photolysis rate constants (k_i), half-lives ($t_{1/2,i}$), and quantum yields (Φ_i) for the different dissociated species of tetracycline antibiotics (TCs)

TCs	Dissociated species (*i*)	k_i (min^{-1})	$t_{1/2,i}$ (min)	Φ_i
TC	H_2TC^0	$(1.19 \pm 0.09) \times 10^{-2}$	58.16 ± 4.66	$(3.48 \pm 0.27) \times 10^{-4}$
	HTC^-	$(2.04 \pm 0.46) \times 10^{-2}$	34.99 ± 7.87	$(5.90 \pm 0.13) \times 10^{-4}$
	TC^{2-}	$(9.38 \pm 0.02) \times 10^{-1}$	0.74 ± 0.02	$(2.87 \pm 0.07) \times 10^{-2}$
OTC	H_2OTC^0	$(2.48 \pm 0.04) \times 10^{-2}$	27.97 ± 0.39	$(5.94 \pm 0.08) \times 10^{-4}$
	$HOTC^-$	$(5.37 \pm 0.74) \times 10^{-2}$	13.02 ± 1.80	$(1.30 \pm 0.18) \times 10^{-3}$
	OTC^{2-}	$(8.59 \pm 0.06) \times 10^{-1}$	0.81 ± 0.01	$(2.28 \pm 0.02) \times 10^{-2}$
CTC	H_2CTC^0	$(2.86 \pm 0.18) \times 10^{-2}$	24.32 ± 1.51	$(8.54 \pm 0.86) \times 10^{-4}$
	$HCTC^-$	$(3.37 \pm 0.35) \times 10^{-2}$	20.69 ± 2.13	$(8.60 \pm 1.89) \times 10^{-4}$
	CTC^{2-}	$(2.68 \pm 5.79) \times 10^{-1}$	2.65 ± 0.57	$(7.60 \pm 0.16) \times 10^{-3}$

of organic compounds, and even for diverse antibiotics in the same class, then $k_{^1O_2,TCs}$ values differed over several orders of magnitude (10^7–10^9).

The $k_{ROS,TCs}$ patterns of TCs reacting with •OH and $^1O_2$ under different pHs are shown in Fig. 2. When the pH increased from 6 to 10, the $k_{ROS,TCs}$ varied greatly. For example, there was a 7-fold variation in $k_{•OH,TCs}$ and 140-fold variation in $k_{^1O_2,TCs}$. Moreover, it can be seen from Fig. 2 that the $^1O_2$ reactivities were highest for the three TCs at pH 10, followed by those at pH 8 and 6. As for •OH oxidation, OTC and CTC showed the fastest reaction when pH was 10, while TC had the highest reactivity at pH 8 when reacting with •OH. The pH dependence was related to the molecular structures and the degree of deprotonation (Mill, 1999; Ge et al., 2019), indicating that there might be differences in the ROS oxidative reactivities of the various dissociated forms of TCs.

Furthermore, the ROS oxidation rate constants of TCs in different dissociated forms ($k_{ROS,i}$) were obtained by matrix calculations, of which the results are shown in Fig. 3 (detailed information in Table A6). It was found that the $k_{ROS,i}$ values differed for the different dissociated forms (H_2TCs^0, $HTCs^-$ and TCs^{2-}) of the individual TCs. The reactivities were highest for OTC and CTC as TCs^{2-} anions, followed by those for the $HTCs^-$ and H_2TCs^0. The TCs^{2-} showed the fastest reaction with $^1O_2$, while $HTCs^-$ had the highest reactivity with •OH. These different reactivities can be attributed to the degree of deprotonation of the TCs. Deprotonation increases the electron density of the compounds and facilitates the electrophilic attack of ROS, promoting the photooxidation reactions (Jiao et al., 2008a). With an increase in pH and hence decline in H^+, the deprotonation of TCs increased, with the proportion of dissociated forms increasing from H_2TCs^0 to TCs^{2-}. Therefore, the photooxidation reactivities of TCs showed a significant dependence on pH and the related dissociated species.

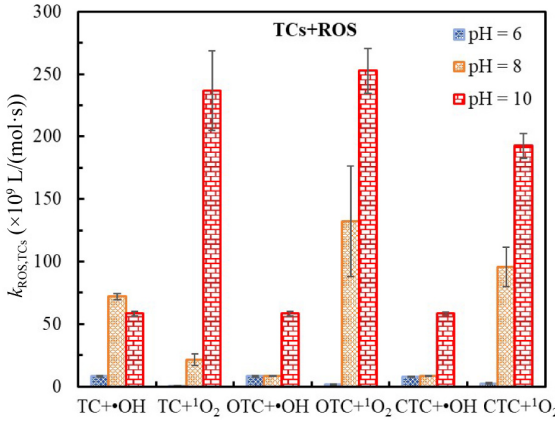

Fig. 2 The aqueous bimolecular rate constants ($k_{•OH,TCs}$ and $k_{1O2,TCs}$) for the reaction between tetracycline antibiotics (TCs) and •OH/$^1O_2$ under different pHs.

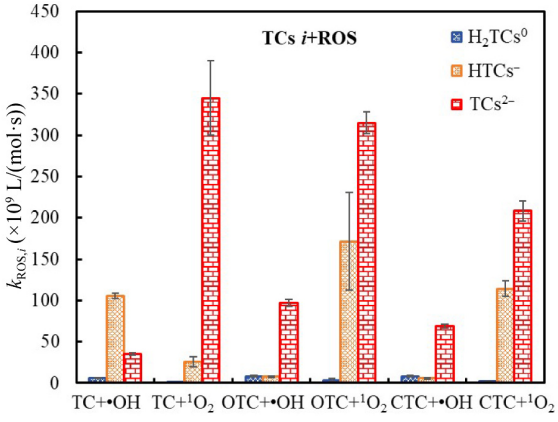

Fig. 3 The bimolecular rate constants ($k_{•OH,\,i}$ and $k_{^1O_{2,i}}$) for the reaction between the different dissociated species (i) of TCs and reactive oxygen species (ROS, •OH and $^1O_2$).

3.3 Photo-transformation half-lives in surface waters

In sunlit surface waters with pH broadly ranging from 6 to 9 (Ge et al., 2019; Zhang et al., 2022c), ionizable organic pollutants usually exist in various dissociated forms, which exhibit different photochemical transformation reactions. Therefore, it is necessary to consider their multiple photo-transformation kinetics to evaluate the total photochemical fate of the pollutants. In the present study, TCs would undergo complex photochemical reactions in surface waters, including sunlit photolysis (rate constants, k_{ap}) and photoinduced ROS oxidation ($k_{oxidation}$), with corresponding multivariate pH-dependent kinetics (Fig. A6 and Table A7). Thus, the corresponding environmental degradation rate constants (k_E) are calculated according to Eqs. (5)–(7),

$$k_E = k_{ap} + k_{oxidation}, \tag{5}$$

$$k_E = 2.303\Phi\sum(L_\lambda\varepsilon_\lambda) + [\bullet OH]k_{•OH,TCs} + [^1O_2]k_{^1O_2,TCs}, \tag{6}$$

$$k_E = 2.303\sum[\delta_i\Phi_i\sum(L_\lambda\varepsilon_{\lambda,i})] + [\bullet OH]\sum(\delta_i k_{•OH,i}) + [^1O_2]\sum(\delta_i k_{^1O_2,i}), \tag{7}$$

where [•OH] and [$^1O_2$] represent the concentrations of •OH and $^1O_2$ in the euphotic zone of surface waters, i.e., [•OH] = 1×10^{-15} mol/L and [$^1O_2$] = 1×10^{-12} mol/L, respectively (Al Housari et al., 2010; Xu et al., 2011). Furthermore, the total environmental photochemical transformation half-lives ($t_{1/2,E}$) in the surface waters can be calculated according to Eq. (8),

$$t_{1/2,E} = \ln 2/k_E. \tag{8}$$

Based on Eqs. (5)–(8), the $t_{1/2,E}$ values of the three TCs were obtained for 45°N latitude assuming continuous solar irradiation (Fig. 4). The values ranged from 0.0624 h for TC in midsummer (pH = 9) to 5.18 h for TC in midwinter (pH = 6), indicating their high dependence on

the water pH and seasonal solar intensity. In direct comparison, the $t_{1/2,E}$ of TCs are comparable to those of furan antibiotics ($t_{1/2,E}$ = 0.08–1.7 h) (Edhlund et al., 2006) and FQs ($t_{1/2,E}$ = 0.03–1.0 h) (Ge et al., 2015), but less than those of SAs ($t_{1/2,E}$ = 6.0–29 h) (Boreen et al., 2004, 2005). The results suggest that these antibiotics degrade quickly in surface waters. However, their continuous release offsets this degradation and probably accounts for their ubiquitous presence in surface waters.

Furthermore, the relative contributions of apparent photolysis and photooxidative degradation to the photochemical degradation of TCs are illustrated in Figs. 5 and A7. In most cases, the apparent photolysis of TCs is the dominant photochemical process, followed by $^1O_2$ and •OH oxidation. In addition, TCs might undergo other minor photo-transformations that are affected by the depth and transparency of water and possibly presence of a wide array of different water constituents (Bodrato and Vione, 2014; Vione et al., 2014). Therefore, to better evaluate the photochemical fate and risk of TCs, further studies were conducted to investigate the transformation pathways and photoinduced toxicity.

3.4 Multiple photo-transformation intermediates and pathways

CTC was selected to reveal the transformation products and pathways for the apparent photolysis, as well as •OH and $^1O_2$ oxidation. The total ion chromatograms obtained in positive ionization mode are shown in Fig. A8. Based on the corresponding fragment information (MS and MS^2 spectra, as shown in Table A8 and Fig. A9), 14 primary intermediates were identified. Their chemical structures and related photo-transformation pathways are illustrated in Fig. 6.

As shown in Fig. 6, there are three different transformation pathways (Paths 1–3), corresponding to the three

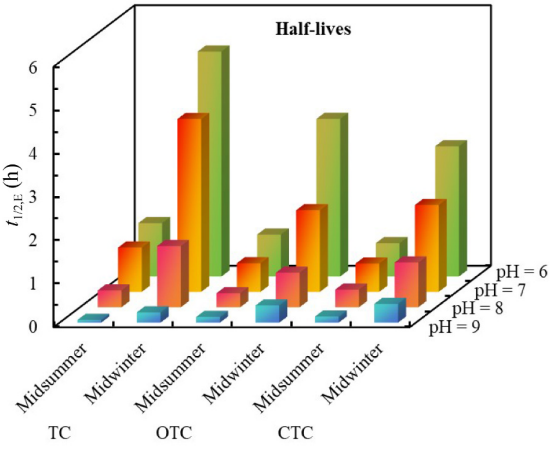

Fig. 4 Multivariate photo-transformation half-lives ($t_{1/2,E}$) of tetracycline antibiotics (TCs) in surface waters with different pH at 45°N latitude.

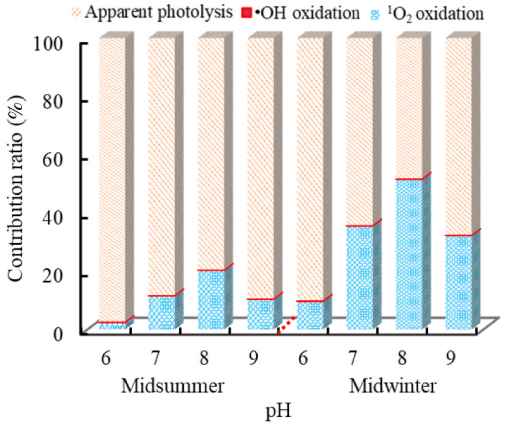

Fig. 5 Relative contributions of apparent photolysis and photooxidative degradation to the photo-transformation of chlortetracycline (CTC) in surface waters at 45°N latitude.

photochemical reactions of CTC (Fig. 4). During the apparent photolysis process (Path 1), CTC was primarily transformed into dechlorinated byproducts (P444) with the loss of –Cl. In Path 2, the •OH oxidation reaction to CTC generated hydroxylated and dechlorinated products, which involved hydroxylation, dehydroxylation, dechlorination, demethylation, and deamidation. These multiple pathways can be attributed to the strong oxidation ability of •OH and the numerous sites in the molecule that are susceptible to •OH attack. As for $^1O_2$ (Path 3), then oxidation, dechlorination, and hydroxylation reactions occurred, as well as a cyclization reaction involved. The cyclization resulted in the generation of the photoproducts (P458, P492, and P510), which were also detected for the photocatalytic degradation of CTC (Liu et al., 2023).

Paths 1–3 compared the multiple photo-transformation intermediates and pathways of CTC, providing fundamental insights into the photochemical fate of the antibiotic pollutant. It is noteworthy that the photolysis and ROS oxidation did not initially affect the core backbone structure of the molecule, so the potential ecotoxicological effects of these primary products might remain and be similar to the parent antibiotics.

3.5 Ecological toxicities of CTC photoproducts

The ecological toxicity of chlortetracycline (CTC) and its photoproducts was evaluated by focusing on their impact on *Vibrio fischeri*, a commonly used bioindicator for environmental toxicity. The results, as depicted in Fig. A10, revealed distinct patterns of toxicity evolution through the different photodegradation pathways. During the apparent photolysis experiments, a significant decrease in solution toxicities was observed ($p < 0.05$), which indicated that the photolysis products of CTC were less toxic than the parent compound. Contrastingly, the photooxidation (•OH and $^1O_2$) processes exhibited a biphasic toxicity pattern: that is an initial decrease

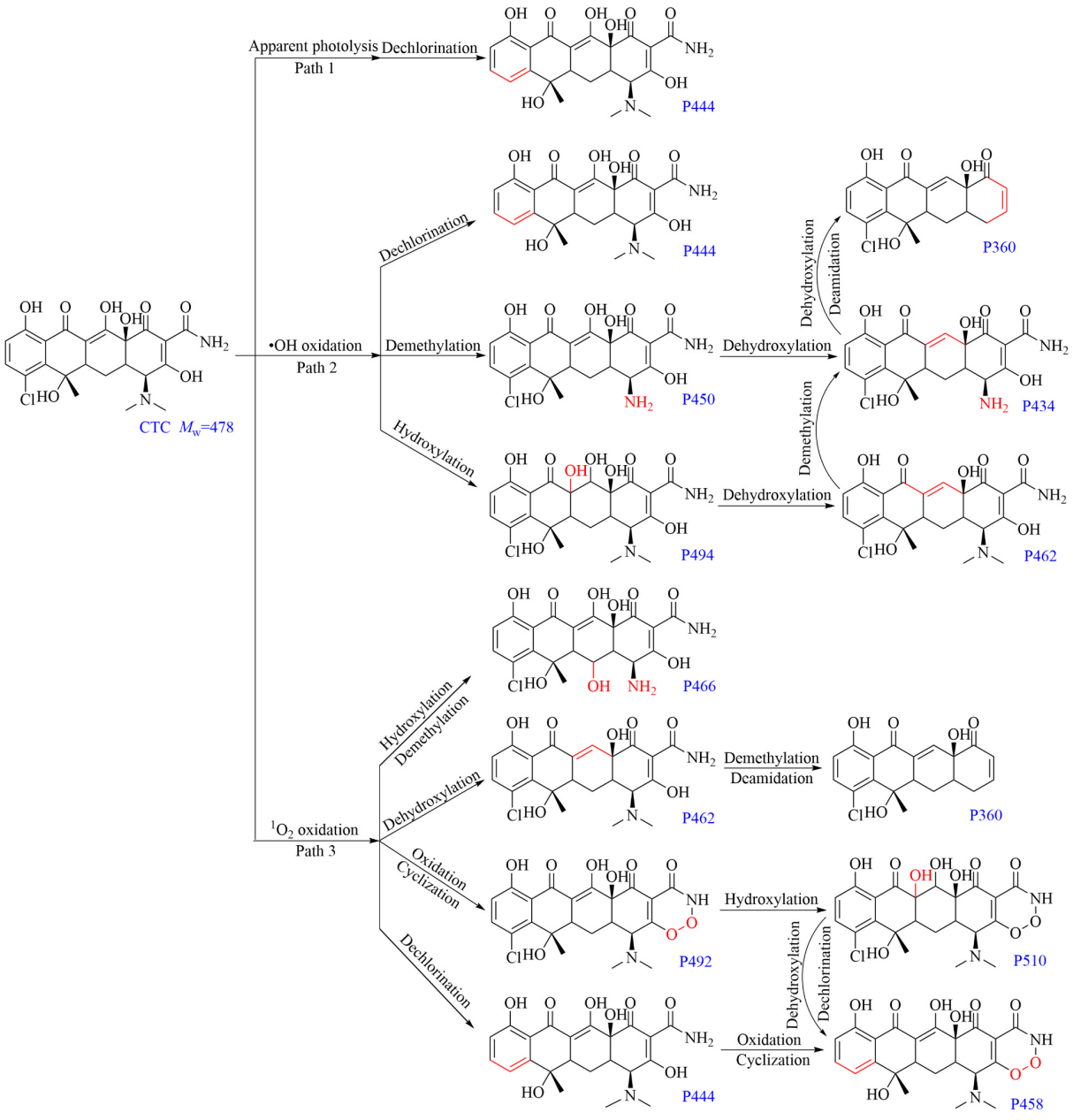

Fig. 6 The main transformation pathways and products for different photochemical reactions of chlortetracycline (CTC). The photoproducts are labeled "P*n*," with *n* for the molecular weights calculated based on the most abundant isotopes.

followed by an increase in toxicity ($p < 0.05$). This indicated the formation of intermediates during the photooxidation that were more toxic than the original CTC. Such an increase in toxicity during photooxidation is a concern as it suggests that while the parent compound is degraded, the byproducts could pose a greater risk to aquatic organisms. Further insights into the toxicity of specific photoproducts were obtained from quantitative toxicity assays. As shown in Table A9, the 96 h LC_{50} (Fish) of CTC was calculated to be 5340.0 mg/L, while the 96 h LC_{50} (Fish) values of P360 and P462 were 11.5 and 777.0 mg/L, respectively. Their 48 h LC_{50} (Daphnid) and 96 h EC_{50} (Green Algae) were also significantly lower than those of the parent compound. This pronounced increase in acute toxicity for the intermediates, particularly P360, is of concern. The formation of more toxic byproducts during photooxidation processes of CTC necessitates careful consideration of the use and management strategies of this antibiotic, especially in aquatic systems that levels of this antibiotic is found to be high.

4 Conclusions

This study provides a comprehensive examination of the degradation kinetics, transformation pathways, and photo-

induced toxicity associated with the photo-transformation reactions of three widely detected TCs in surface waters. Notably, apparent photolysis, as well as •OH and $^1O_2$ photooxidation, was significantly influenced by the presence of the major dissociated forms of TCs (H_2TCs^0, $HTCs^-$, and TCs^{2-}), which in turn is dependent on the pHs. The acceleration of their apparent photolysis with increasing pH values was attributed to incremental rate constants and quantum yields from H_2TCs^0 to TCs^{2-}. Moreover, different dissociated forms of TCs exhibited distinct reactivities toward •OH and $^1O_2$, which were closely linked to their degree of deprotonation. This highlights the importance of understanding the chemical nature of contaminants in predicting their behavior under environmental conditions. Considering the reactivities of these dissociated species, the environmental photo-transformation half-lives of TCs in sunlit surface waters displayed a pronounced dependence on water pH and seasonal variations. These factors are crucial in predicting the persistence of TCs in different aquatic environments and must be considered in environmental monitoring and modeling. Importantly, the three reactions led to the generation of multiple intermediates and distinct primary transformation pathways involving dechlorination, hydroxylation, and cyclization, respectively. The formation of more toxic intermediates during •OH and $^1O_2$ photooxidation processes gives rises to concerns regarding the presence of these chemicals in the wider aquatic environment. These intermediates demonstrated photomodified toxicities that were higher than the parent compounds. The identification of these toxic intermediates calls for a reevaluation of water treatment processes and their efficacy in not just removing, but also in detoxifying water contaminants. The insights from this study are paramount for improving the understanding of TC photo-transformation during wastewater treatment and in natural aquatic environments. These findings will help improve risk assessment processes concerning the use, release and impact of TCs on non-target organisms in aquatic systems.

Acknowledgements This work was supported by the Key Research and Development Program of Shaanxi Province (No. 2024SF-YBXM-567), the National Natural Science Foundation of China (Nos. 21976045 and 22076112), the China Scholarship Council (CSC) Scholarship (No. 202308610123), and the Shaanxi Key Laboratory of Environmental Monitoring and Forewarning of Trace Pollutants (No. SHJKFJJ202318).

Conflict of Interests The authors declare that the research was conducted in the absence of any commercial or financial relationships that could be construed as a potential conflict of interest.

Electronic Supplementary Material Supplementary material is available in the online version of this article at https://doi.org/10.1007/s11783-024-1899-x and is accessible for authorized users.

References

Adamek E, Baran W, Sobczak A (2016). Assessment of the biodegradability of selected sulfa drugs in two polluted rivers in Poland: effects of seasonal variations, accidental contamination, turbidity and salinity. Journal of Hazardous Materials, 313: 147–158

Al Housari F, Vione D, Chiron S, Barbati S (2010). Reactive photoinduced species in estuarine waters: characterization of hydroxyl radical, singlet oxygen and dissolved organic matter triplet state in natural oxidation processes. Photochemical & Photobiological Sciences, 9(1): 78–86

An J, Chen H, Wei S, Gu J (2015). Antibiotic contamination in animal manure, soil, and sewage sludge in Shenyang, northeast China. Environmental Earth Sciences, 74(6): 5077–5086

Anjali R, Shanthakumar S (2019). Insights on the current status of occurrence and removal of antibiotics in wastewater by advanced oxidation processes. Journal of Environmental Management, 246: 51–62

Bodrato M, Vione D (2014). APEX (Aqueous photochemistry of environmentally occurring xenobiotics): a free software tool to predict the kinetics of photochemical processes in surface waters. Environmental Science. Processes & Impacts, 16(4): 732–740

Boreen A L, Arnold W A, Mcneill K (2004). Photochemical fate of sulfa drugs in the aquatic environment: sulfa drugs containing five-membered heterocyclic groups. Environmental Science & Technology, 38(14): 3933–3940

Boreen A L, Arnold W A, Mcneill K (2005). Triplet-sensitized photodegradation of sulfa drugs containing six-membered heterocyclic groups: identification of an SO_2 extrusion photoproduct. Environmental Science & Technology, 39(10): 3630–3638

Chen W, Huang C (2011). Transformation kinetics and pathways of tetracycline antibiotics with manganese oxide. Environmental Pollution, 159(5): 1092–1100

Chen Y, Li H, Wang Z, Tao T, Hu C (2011). Photoproducts of tetracycline and oxytetracycline involving self-sensitized oxidation in aqueous solutions: effects of Ca^{2+} and Mg^{2+}. Journal of Environmental Sciences, 23(10): 1634–1639

Cheng J, Jiang L, Sun T, Tang Y, Du Z, Lee L, Zhao Q (2019). Occurrence, seasonal variation and risk assessment of antibiotics in the surface water of north China. Archives of Environmental Contamination and Toxicology, 77(1): 88–97

Edhlund B L, Arnold W A, Mcneill K (2006). Aquatic photochemistry of nitrofuran antibiotics. Environmental Science & Technology, 40(17): 5422–5427

Felis E, Buta-Hubeny M, Zieliński W, Hubeny J, Harnisz M, Bajkacz S, Korzeniewska E (2022). Solar-light driven photodegradation of antimicrobials, their transformation by-products and antibiotic resistance determinants in treated wastewater. Science of the Total Environment, 836: 155447

Ge L, Chen J, Wei X, Zhang S, Qiao X, Cai X, Xie Q (2010). Aquatic photochemistry of fluoroquinolone antibiotics: kinetics, pathways, and multivariate effects of main water constituents. Environmental Science & Technology, 44(7): 2400–2405

Ge L, Halsall C, Chen C, Zhang P, Dong Q, Yao Z (2018). Exploring the aquatic photodegradation of two ionisable fluoroquinolone antibiotics-gatifloxacin and balofloxacin: degradation kinetics, photobyproducts and risk to the aquatic environment. Science of the Total Environment, 633: 1192–1197

Ge L, Na G, Zhang S, Li K, Zhang P, Ren H, Yao Z (2015). New insights into the aquatic photochemistry of fluoroquinolone antibiotics: direct photodegradation, hydroxyl-radical oxidation, and antibacterial activity changes. Science of the Total Environment, 527-528: 12-17

Ge L, Zhang P, Halsall C, Li Y, Chen C, Li J, Sun H, Yao Z (2019). The importance of reactive oxygen species on the aqueous phototransformation of sulfonamide antibiotics: kinetics, pathways, and comparisons with direct photolysis. Water Research, 149: 243–250

Guo H, Chen Z, Lu C, Guo J, Li H, Song Y, Han Y, Hou Y (2020). Effect and ameliorative mechanisms of polyoxometalates on the denitrification under sulfonamide antibiotics stress. Bioresource Technology, 305: 123073

Han C H, Park H D, Kim S B, Yargeau V, Choi J W, Lee S H, Park J A (2020). Oxidation of tetracycline and oxytetracycline for the photo-Fenton process: their transformation products and toxicity assessment. Water Research, 172: 115514

He Y, Yuan Q, Mathieu J, Stadler L, Senehi N, Sun R, Alvarez P J (2020). Antibiotic resistance genes from livestock waste: occurrence, dissemination, and treatment. npj Clean Water, 3(1): 4

Hu S, Zhang H, Yang Y, Cui K, Ao J, Tong X, Shi M, Wang Y, Chen X, Li C, et al. (2024). Comprehensive insight into the occurrence characteristics, influencing factors and risk assessments of antibiotics in the Chaohu Basin. Frontiers of Environmental Science & Engineering, 18(5): 57–71

Jiao S, Zheng S, Yin D, Wang L, Chen L (2008a). Aqueous oxytetracycline degradation and the toxicity change of degradation compounds in photoirradiation process. Journal of Environmental Sciences, 20(7): 806–813

Jiao S, Zheng S, Yin D, Wang L, Chen L (2008b). Aqueous photolysis of tetracycline and toxicity of photolytic products to luminescent bacteria. Chemosphere, 73(3): 377–382

Jin X, Xu H, Qiu S, Jia M, Wang F, Zhang A, Jiang X (2017). Direct photolysis of oxytetracycline: Influence of initial concentration, pH and temperature. Journal of Photochemistry and Photobiology A Chemistry, 332: 224–231

Knapp C, Cardoza L, Hawes J, Wellington E, Larive C, Graham D (2005). Fate and effects of enrofloxacin in aquatic systems under different light conditions. Environmental Science & Technology, 39(23): 9140–9146

Latch D E, Packer J L, Stender B L, Vanoverbeke J, Arnold W A, Mcneill K (2005). Aqueous photochemistry of triclosan: formation of 2,4-dichlorophenol, 2,8-dichlorodibenzo-*p*-dioxin, and oligomerization products. Environmental Toxicology and Chemistry, 24(3): 517–525

Li R, Zhao C, Yao B, Li D, Yan S, O'Shea K E, Song W (2016). Photochemical transformation of aminoglycoside antibiotics in simulated natural waters. Environmental Science & Technology, 50(6): 2921–2930

Li S, Shi W, Liu W, Li H, Zhang W, Hu J, Ke Y, Sun W, Ni J (2018). A duodecennial national synthesis of antibiotics in China's major rivers and seas (2005–2016). Science of the Total Environment, 615: 906–917

Li T, Ouyang W, Lin C, Wang J, Cui X, Li Y, Guo Z, Zhu W, He M (2023). Occurrence, distribution, and potential ecological risks of antibiotics in a seasonal freeze-thaw basin. Journal of Hazardous Materials, 459: 132301

Liu H, Niu C, Huang D, Liang C, Guo H, Yang Y, Li L (2023). Unravelling the role of reactive oxygen species in ultrathin Z-scheme heterojunction with surface zinc vacancies for photocatalytic H_2O_2 generation and CTC degradation. Chemical Engineering Journal, 465: 143007

Liu X, Lu S, Guo W, Xi B, Wang W (2018). Antibiotics in the aquatic environments: a review of lakes, China. Science of the Total Environment, 627: 1195–1208

Liu Y, Mekic M, Carena L, Vione D, Gligorovski S, Zhang G, Jin B (2020). Tracking photodegradation products and bond-cleavage reaction pathways of triclosan using ultra-high resolution mass spectrometry and stable carbon isotope analysis. Environmental Pollution, 264: 114673

Mill T (1999). Predicting photoreaction rates in surface waters. Chemosphere, 38(6): 1379–1390

Niu J, Li Y, Wang W (2013). Light-source-dependent role of nitrate and humic acid in tetracycline photolysis: kinetics and mechanism. Chemosphere, 92(11): 1423–1429

Oka H, Ikai Y, Kawamura N, Yamada M, Harada K, Ito S, Suzuki M (1989). Photodecomposition products of tetracycline in aqueous solution. Journal of Agricultural and Food Chemistry, 37(1): 226–231

Park J A, Pineda M, Peyot M L, Yargeau V (2023). Degradation of oxytetracycline and doxycycline by ozonation: degradation pathways and toxicity assessment. Science of the Total Environment, 856: 159076

Ping Q, Yan T, Wang L, Li Y, Lin Y (2022). Insight into using a novel ultraviolet/peracetic acid combination disinfection process to simultaneously remove antibiotics and antibiotic resistance genes in wastewater: mechanism and comparison with conventional processes. Water Research, 210: 118019

Qi N, Wang P, Wang C, Ao Y (2018). Effect of a typical antibiotic (tetracycline) on the aggregation of TiO_2 nanoparticles in an aquatic environment. Journal of Hazardous Materials, 341: 187–197

Riu A, Le Maire A, Grimaldi M, Audebert M, Hillenweck A, Bourguet W, Balaguer P, Zalko D (2011). Characterization of novel ligands of ERα, Erβ, and PPARγ: the case of halogenated bisphenol A and their conjugated metabolites. Toxicological Sciences, 122(2): 372–382

Sciscenko I, Arques A, Varga Z, Bouchonnet S, Monfort O, Brigante M, Mailhot G (2021). Significant role of iron on the fate and photodegradation of enrofloxacin. Chemosphere, 270: 129791

Song C, Liu H, Guo S, Wang S (2020). Photolysis mechanisms of tetracycline under UV irradiation in simulated aquatic environment surrounding limestone. Chemosphere, 244: 125582

Su Z, Wang K, Yang F, Zhuang T (2023). Antibiotic pollution of the Yellow River in China and its relationship with dissolved organic matter: distribution and source identification. Water Research, 235: 119867

Tian Y, Ying C, Zhang L, Huang H, Song S, Mei R, Li J (2024). Unveiling the inhibition of chlortetracycline photodegradation and the increase of toxicity when coexisting with silver nanoparticles. Science of the Total Environment, 912: 168443

Tran N H, Hoang L, Nghiem L D, Nguyen N M H, Ngo H H, Guo W,

Trinh Q T, Mai N H, Chen H, Nguyen D D, et al. (2019). Occurrence and risk assessment of multiple classes of antibiotics in urban canals and lakes in Hanoi, Vietnam. Science of the Total Environment, 692: 157–174

Vione D, Minella M, Maurino V, Minero C (2014). Indirect photochemistry in sunlit surface waters: photoinduced production of reactive transient species. Chemistry, 20(34): 10590–10606

Wang Q, He X, Xiong H, Chen Y, Huang L (2022). Structure, mechanism, and toxicity in antibiotics metal complexation: recent advances and perspectives. Science of the Total Environment, 848: 157778

Werner J J, Arnold W A, Mcneill K (2006). Water hardness as a photochemical parameter: tetracycline photolysis as a function of calcium concentration, magnesium concentration, and pH. Environmental Science & Technology, 40(23): 7236–7241

Xu H, Cooper W J, Jung J, Song W (2011). Photosensitized degradation of amoxicillin in natural organic matter isolate solutions. Water Research, 45(2): 632–638

Xu L, Zhang H, Xiong P, Zhu Q, Liao C, Jiang G (2021a). Occurrence, fate, and risk assessment of typical tetracycline antibiotics in the aquatic environment: a review. Science of the Total Environment, 753: 141975

Xu T, Fang Y, Tong T, Xia Y, Liu X, Zhang L (2021b). Environmental photochemistry in hematite-oxalate system: Fe (III)-Oxalate complex photolysis and ROS generation. Applied Catalysis B: Environmental, 283: 119645

Ye C, Chen Y, Feng L, Wan K, Li J, Feng M, Yu X (2022). Effect of the ultraviolet/chlorine process on microbial community structure, typical pathogens, and antibiotic resistance genes in reclaimed water. Frontiers of Environmental Science & Engineering, 16(8): 100–113

Yu J, Chen X, Zhang Y, Cui X, Zhang Z, Guo W, Wang D, Huang S, Chen Y, Hu Y, et al. (2022). Antibiotic azithromycin inhibits brown/beige fat functionality and promotes obesity in human and rodents. Theranostics, 12(3): 1187–1203

Yuan X, Cui K, Chen Y, Wu S, Zhang Y, Liu T (2023). Response of antibiotic and heavy metal resistance genes to the co-occurrence of gadolinium and sulfamethoxazole in activated sludge systems. Frontiers of Environmental Science & Engineering, 17(12): 154–164

Zhang C, Chen Y, Chen S, Guan X, Zhong Y, Yang Q (2023). Occurrence, risk assessment, and *in vitro* and *in vivo* toxicity of antibiotics in surface water in China. Ecotoxicology and Environmental Safety, 255: 114817

Zhang M, He L, Liu Y, Zhao J, Liu W, Zhang J, Chen J, He L, Zhang Q, Ying G (2019). Fate of veterinary antibiotics during animal manure composting. Science of the Total Environment, 650: 1363–1370

Zhang T, Cheng F, Yang H, Zhu B, Li C, Zhang Y N, Qu J, Peijnenburg W J (2022a). Photochemical degradation pathways of cell-free antibiotic resistance genes in water under simulated sunlight irradiation: experimental and quantum chemical studies. Chemosphere, 302: 134879

Zhang X, Kamali M, Yu X, Costa M E V, Appels L, Cabooter D, Dewil R (2022b). Kinetics and mechanisms of the carbamazepine degradation in aqueous media using novel iodate-assisted photochemical and photocatalytic systems. Science of the Total Environment, 825: 153871

Zhang X, Su H, Gao P, Li B, Feng L, Liu Y, Du Z, Zhang L (2022c). Effects and mechanisms of aged polystyrene microplastics on the photodegradation of sulfamethoxazole in water under simulated sunlight. Journal of Hazardous Materials, 433: 128813

Zhang Y, Zhang C, Parker D B, Snow D D, Zhou Z, Li X (2013). Occurrence of antimicrobials and antimicrobial resistance genes in beef cattle storage ponds and swine treatment lagoons. Science of the Total Environment, 463-464: 631-638

Zheng J, Zhang P, Li X, Ge L, Niu J (2023). Insight into typical photo-assisted AOPs for the degradation of antibiotic micropollutants: mechanisms and research gaps. Chemosphere, 343: 140211

Zhou Y, Cheng F, He D, Zhang Y, Qu J, Yang X, Chen J, Peijnenburg W J (2021). Effect of UV/chlorine treatment on photophysical and photochemical properties of dissolved organic matter. Water Research, 192: 116857